
A new parsimonious method for classifying Cancer Tissue-of-Origin Based on DNA Methylation 450K data

Shen Jia^{1#}, Yulin Zhang^{2#}, Yiming Mao¹, Jiawei Gao¹, Yixuan Chen¹,

Yuxuan Jiang¹, Haochen Luo³, Kebo Lv^{4*}, Jionglong Su^{5*}

¹ *Department of Mathematics, University of Liverpool, Liverpool, UK*

² *College of Mathematics and Systems Science, Shandong University of Science and Technology, Qingdao, China*

³ *Department of Computer Science, University of Liverpool, UK*

⁴ *School of Mathematical Sciences, Ocean University of China, Qingdao, China*

⁵ *School of AI and Advanced Computing, XJTLU Entrepreneur College(Taicang), Xi'an Jiaotong-Liverpool University, Suzhou, China*

These authors contribute equally to the work

***Corresponding author: Kebo Lv (e-mail: kewave@ouc.edu.cn),
Jionglong Su (email: Jionglong.Su@xjtlu.edu.cn)**

Abstract

DNA methylation is a well-studied genetic modification that regulates gene transcription of Eukaryotes. Its alternations have been recognized as a significant component of cancer development. In this study, we use the DNA methylation 450k data from The Cancer Genome Atlas to evaluate the efficacy of DNA methylation data on cancer classification for 30 cancer types. We propose a new method for gene selection in high dimensional data(over 450 thousand). Variance filtering is first introduced for dimension reduction and Recursive feature elimination (RFE) is then used for feature selection. We address the problem of selecting a small subsets of genes from large number of methylated sites, and our parsimonious model is demonstrated to be efficient, achieving an accuracy over 91%, outperforming other studies which use DNA micro-arrays and RNA-seq Data . The performance of 20 models, which are based on 4 estimators (Random Forest, Decision Tree, Extra Tree and Support Vector Machine) and 5 classifiers (k-Nearest Neighbours, Support Vector Machine, XGboost, Light GBM and Multi-Layer Perceptron), is compared and robustness of the RFE algorithm is examined. Results suggest that the combined model of extra tree plus catboost classifier offers the best performance in cancer identification, with an overall validation accuracy of 91% , 92.3%, 93.3% and 93.5% for 20, 30, 40 and 50 features respectively. The biological functions in cancer development of 50 selected genes is also explored through enrichment analysis and the results show that 12 out of 16 of our top features have already been identified to be specific with cancer and we also propose some more genes to be tested for future studies. Therefore, our method may be utilized as an auxiliary diagnostic method to determine the actual clinicopathological status of a specific cancer.

1 Introduction

1.1 DNA methylation and cancer identification

DNA methylation is an epigenetic modification of the genome that is crucial for the normal regulation of gene transcription [1]. It is a biological process involving the transfer of a methyl group onto the C5 position of the cytosine to form 5-methylcytosine [2]. In normal cells, this modification results in different interaction properties assuring the proper regulation of gene expression and of gene silencing [3]. In contrast, malignant cells show major disruptions in their DNA methylation patterns. Alternations of DNA methylation consist of hypomethylation and hypermethylation have been recognized as an important component of cancer development. (Hypomethylation is usually linked to activation of oncogenes, whereas hypermethylation of the CpG islands is associated with silencing of cancer suppressor gene [4].) With the DNA methylation profile, it is expected that classification of cancer can be achieved based on different levels of DNA methylation, which may be helpful in tumor diagnosis and drug development [1,5]. Generally, it is known that cancer is a group of diseases that are driven by progressive genetic abnormalities that include mutations in tumor-suppressor genes and oncogenes, as well as chromosomal abnormalities [6]. While the role of genetic mutations has been highlighted by many researchers [7-11], epigenetic alternations such as DNA methylation have also been found highly related to cancer development [12].

Traditionally, cancer identification is carried out through medical tests such as lab tests, imaging tests and biopsy [13]. Previous work of Masilamani et.al [14] suggests that lab tests such as blood tests for tumor markers have great potential for early detection of cancer. However, as pointed out by National Cancer Institutes (NCI), abnormal lab results are not a sure sign of cancer and most of them may only be helpful in assessment of cancer risk rather than diagnosis [15]. Likewise, imaging tests are helpful in the early detection of cancer. They can help locate and find out the stage of the tumor. However, due to some similar appearance between cancer

and other types of diseases, they are not suitable for making a final diagnosis. Additionally, since it takes millions of cells to make a tumor big enough to appear on an imaging test, imaging test may only be helpful in detecting large groups of cancer cells [16]. In terms of biopsies, although they provide the most accurate diagnosis of cancer, a sample is needed to run such tests. Usually, the biopsy sample is obtained with a needle, endoscopy or even a surgery and these may cause great pain to patients [13].

Considering the limitations of current techniques, we hope to provide additional tools for cancer identification and classification from a molecular level using sequencing DNA methylation data. The genetic analysis of methylated DNA data may also provide new insights into drug development.

1.2 Sequencing data improves cancer classification

Accurately identifying specific cancer holds great promise for further treatment selection and prediction of prognosis in cancer [12]. However, due to the limitations of surgical tolerance in patients, it might be difficult for the surgeons to use complex anatomy to obtain cancer diagnosis in high accuracy [17]. Sometimes, even when the tumors are successfully obtained, similar histopathological appearance of different tumors may still lead to misdiagnosis and consequently treatment may not achieve effective therapeutic effect [18]. The uncertainty of this kind of prognosis propels the development of other diagnostic approaches with higher certainty. With the improvement of the Next-Generation Sequencing (NGS) technology, more and more sequencing data e.g., DNA-seq, RNA-seq are available to researchers which require advanced methods to mine these data and provide a more general and reliable information for clinical diagnosis [19] through specific biological insights. A great number of research have been carried out for classifying cancer types and subtypes using sequencing data. For instance, Li(2017) and his team, who used the RNA-seq Data to extract 20 features in the classification of 33 different types of tumors with the mean of ML, with the final accuracy rate exceeded 90% [20]. Similar thoughts

could be seen from Zhang (2018)'s project, where they proposed a prognosis model based on Bayesian network classification of breast tumor with 888 features extracted from DNA methylation Data [21]. Raweh (2018) and his team used TCGA data sets and RnRead software to extract the 512 useful feature from the raw data, then utilized the method of fast Fourier transform algorithm for seven types of cancer respectively extracted less than 10 corresponding characteristics and finally used different classifiers (such as random forest) and support vector machine to get an overall accuracy which was above 97% [22]. However, despite the fact that many techniques have been applied to analyze gene expression data, it has been demonstrated by previous studies that some common machine learning methods such as Support Vector Machine may not perform well due to the high dimensionality and small sample size of Gene Expression Profiles (GEP) dataset [23]. Thus, the design of dimensional reduction method to drastically reduce the number of features in sequencing data would be the key to acquire a model in high accuracy.

1.3 Our work

In this study, we use the DNA methylation 450k data from The Cancer Genome Atlas to evaluate the efficacy of DNA methylation data on cancer classification for 30 cancer types. Since the dimension of the data is extremely high(over 450 thousand), we first use the variance selection method to reduce dimension and then utilize the recursive feature elimination algorithm to extract the features. Enrichment analysis is then carried out to explore the biological meaning of the selected genes.

1.3.1 Motivation

The motivation of this paper is two-fold:

(i) First, inspired by Darst who acknowledged the positive impact of Random Forest-Recursive Feature Elimination algorithm in extracting features from smaller data sets, our team apply the algorithm into high dimensional data[24].

(ii) Second, the 450k methylation value provides a genome-wide quantitative representation of DNA methylation value in a convenient format, which makes the data preprocessing process for analysts easier and more feasible and thus arouses our interest to explore its correlation with cancer[25].

1.3.2 Novelty

The novelty of this paper is three-fold:

(i) First, many previous works[20,21] dived into the area where the sequencing data was used to diagnosing cancer type, but to the best of our knowledge, none of them focused on the DNA methylation 450k data to carry out the cancer classification.

(ii) Second, instead of building a model with hundreds of identifiers like Zhang (2018) and Raweh (2017) did, our team focus on the feasibility to construct a parsimonious model with relatively fewer number of identifiers (within 50 features).

(iii) Third, we propose a novel method which includes variance selection, recursive feature elimination and boosting classifiers in extracting features from high dimensional data.

1.3.3 Key contributions

The key contributions of this paper are two-fold:

First, we have demonstrated the efficiency of our parsimonious model, with an overall accuracy of 91% , 92.3%, 93.3% and 93.5% for 20, 30, 40 and 50 features respectively, achieving the same level of accuracies of over 90% as other studies which use DNA micro-arrays and RNA-seq Data.

Second, 12 out of 16 top features in our studies have been already shown to play a part in cancer development, and we thus recommend some more genes for further testing.

This paper is divided into four sections as follows:

- 1) Section I is the introduction. It briefly describes the background of the cancer identification and the significance of DNA methylation for cancer identification .
- 2) Section II contains methodology. This part mainly introduces the source of the dataset and how our work is conducted in the two phases: dimensionality reduction and feature selection.
- 3) Section III Results and Discussions. This chapter presents the result of our algorithm and compared the performance of models with different number of features and classifiers. At the same time, it also includes enrichment analysis and gene annotations to explore the biology meaning of our works
- 4) Section IV contains the conclusion of this article and the work we expect to do in the future.

2 Methodology

2.1 Dataset

The Cancer Genome Atlas (TCGA) is a landmark project led by the National Cancer Institute (NCI) and National Human Genome Research Institute (NHGRI) that aims to catalogue major cancer-causing genetic mutations [26]. The TCGA dataset, molecularly characterized over 20,000 primary cancer and matched normal samples spanning over 30 cancer types, is publicly available [27, 28].

This study focuses on the DNA methylation data from the TCGA dataset provided by UCSC Xena. DNA methylation profile was obtained using the Illumina Infinium HumanMethylation450 platform which includes more than 450 thousand CpG site probes(HumanMethylation450), which provides quantitative methylation measurement at the single-CpG-site level. Featuring more than 450 thousand methylation sites, the Infinium HumanMethylation450 BeadChip offers a

combination of comprehensive, expert-selected coverage and high throughput at a low price, thus enabling cost-effective DNA methylation analysis for a variety of applications [29]. Due to its comprehensive genome-wide coverage as well as incomparable cost-effectiveness, the HumanMethylation450 datasets have become a popular choice for the study of epigenetic changes in many diseases processes [29-31]. Saumya used DNA Methylation 450K data to reveal the peripheral blood differential methylation in male infertility and Bonnie utilized the same data to make the MGMT mrthylation assessment in glioblastoma[32,33].

In this study, the methylation 450kdata we use derived from UCSC Xena has already gone through quality control such as filtration of low quality probes as well as normalization process and DNA methylation level is measured in beta value defined as the ratio of the methylated probe intensity and the overall intensity (sum of methylated and unmethylated probe intensities) [34].

$$\beta_n = \frac{\max(Meth_n, 0)}{\max(Meth_n, 0) + \max(Unmeth_n, 0) + \alpha}$$

which is a continuous variable between 0 and 1. Higher beta value represents higher level of DNA methylation whereas lower beta value represents lower level of DNA methylation.

2.2 Dimension Reduction

The study focuses on 30 DNA methylation datasets extracted from TCGA (listed in Table 1). The original data consists of over 450 thousand identifiers representing the ID number of the probes and 9743 samples in total, with a number of features containing missing value due to low quality of certain Methylation450 BeadChip probes.

Inspired by the idea of neural network, the feature selection from the original 480,000 CpG sites is implemented in two-phases (*Figure 1*). we propose a 'hidden-layer' (Medium Layer) size features which is the output of the variance selection

(Dimension Reduction) as well as the input of the latter RFE[35] process (Feature Selection).

In the first step, by variance selection method (Dimension Reduction), we reduce the number 450,000 to 2000 features.

In the second step, the first phase's output becomes the input of the RFE process (Feature Selection) and we extract 20 features from the 2000 CpG sites, which will be later discussed in 2.3. The reason we construct a 'hidden-layer' here is that though RFE can provide precise solution, the time overhead is a defect when the input features are enormous[35]. In addition, if we directly apply RFE algorithm to 480,000 features, the algorithm's stability is questioned since redundant and noisy genes are not removed at first as Tang proved [36].

Before the dimensionality reduction and feature selection, features with missing values in the samples were removed and then 30 datasets were merged into one overall dataset.

After that, Dimension reduction was conducted based on variance between and within different cancer groups . Afshar(2020) demonstrated the effectiveness of removing features with low variance so as to select important features in high dimensional data [37]and Model(2001) showed that genes with large variance are more important features since they explain most of the total variances[38].

Therefore, we combined their thoughts and applied the variance selection in this study.

The following are the formulas of the within groups variance $s_{n,j}^2$ and between groups variance S_j^2 respectively. In formula (1), $x_{i,j}^{(n)}$ represents the value in row(Sample) i and column(feature) j of n th class. In addition, $\bar{x}_j^{(n)}$ represents the mean of all the values in column(feature) j of n th class. N_n represent the number of sample each cancer class has. Similarly, in the latter, $x_{i,j}$ represents the value in row(Sample) i and column(feature) j , \bar{x}_j represents the mean of all the values in column(feature) j . N represents the number of total samples.

$$S_{n,j}^2 = \sum_{i=1}^{N_n} \frac{(x_{i,j}^{(n)} - \bar{x}_j^{(n)})^2}{N_n - 1} \quad (1)$$

$$S_j^2 = \sum_{i=1}^N \frac{(x_{i,j} - \bar{x}_j)^2}{N - 1} \quad (2)$$

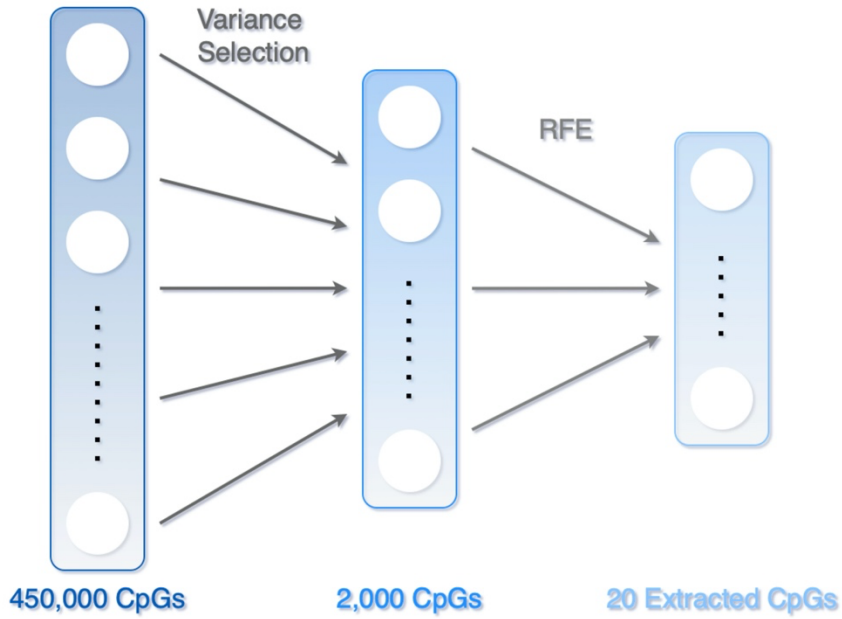


FIGURE 1 | Dimension Reduction and Feature Selection

Figure 1 Dimension Reduction and Feature Selection

2.3 Features selection

In this part, we mainly utilize the feature selection algorithm recursive feature elimination method (RFE) method[35] to obtain the most important features from a total of 2000 identifiers after the first step. As the work of Guyon et.al [35] illustrates, this algorithm achieve high accuracy in genetic diagnosis and gene selection. More specifically, RFE is a method for feature selection which selects features by recursively obtaining increasingly smaller sets of features until gets the required number of features. An estimator, namely a classifier gives the importance of the features, is an essential part of this algorithm, which computes the

significance of the features. In each loop, it ranks the significance of the features and eliminates the worst feature. Here, we choose accuracy as the indicator for the RFE and mainly tune the number of chosen features to compare the results.

Since the RFE method is estimator bounded, the choice of it can be vital. According to Deng(2012), tree-based classifiers are frequently chosen as the estimator since they can provide variable significance scores and perform relatively strong[39].

Similar points can be seen in Touw(2013) 's paper, which demonstrates the significance of random forest classifier to the bioinformatics area[40]. Therefore, random forest are chosen in this paper as the estimator and we also proposed its similar algorithm decision tree [41] and extra tree [42] to be tested.

On the other hand, Moon(2016) demonstrated that the L1-norm SVM performed well as the feature selection estimators when dealing with the biomedical data[43]. Reasons are that the figure for the biostatisticians tend to be centered in an interval which can be hard to distinguish while L1-based classifiers are able to make them sparse and easier for detect. As a result, since the data we have are the decimals between 0.0 and 1.0(mainly 0.1 to 0.9 according to the information on <https://xenabrowser.net>) , we follow Moon and his team to use the L1-norm SVM as the estimator

Therefore, we aim to use these four estimators to get the scores for each feature and then select the top several to feed into the classifiers. To mention above, five different classifiers are used in this paper. Following Sahu(2017) 's research[44] on the DNA microarray data, Support Vector machines (SVM) [45], k-Nearest Neighbors (KNN) [46] and Multilayer Perceptron (MLP) 2.3[47] are chosen. Besides, another two ensemble classifiers LightGBM [48] and Xgboost[49] are also used.

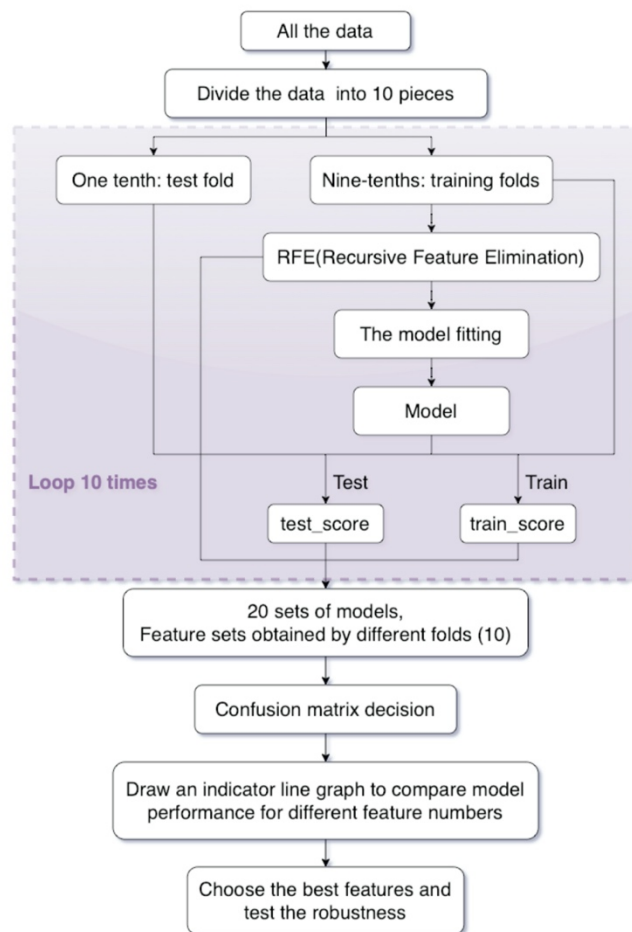


FIGURE 2 | Flow chart of method

The feature set filtered by variance was first divided into 10 parts for 10 folds cross validation(Figure 2). In each iteration, keep one fold of the data as the validation set and use the other 9 parts as the training set. Then we use the RFE method to fit on the training set and achieve the selected features. Thus, a new subset of the data, written by using the selected CpG sites as features, enters into the classifier to be evaluated. Here, the key point is that we need to check the performance of the selected features as well as choosing the best group (features plus the classifier) as the final model.

Since there are four estimators as well as five various classifiers in the experiment, a total number of 20 groups are made and each group contains 10 iterations since a ten folds cross-validation is contained in each group. As shown in the graph(Figure 3), the training set and test set were tested respectively with the models (the motion

for testing the training part is to check whether the model is overfitting), and the accuracy was recorded at intervals of 10 features from 20 to 50. In this way, two lists each containing train score and test score respectively are obtained. Therefore, for each of the 20 models, we obtained accuracy for each folds on the validation set and averaged them to get one mean set accuracy for the different number of features as well as calculated the minimum and maximum value of the 10 groups.

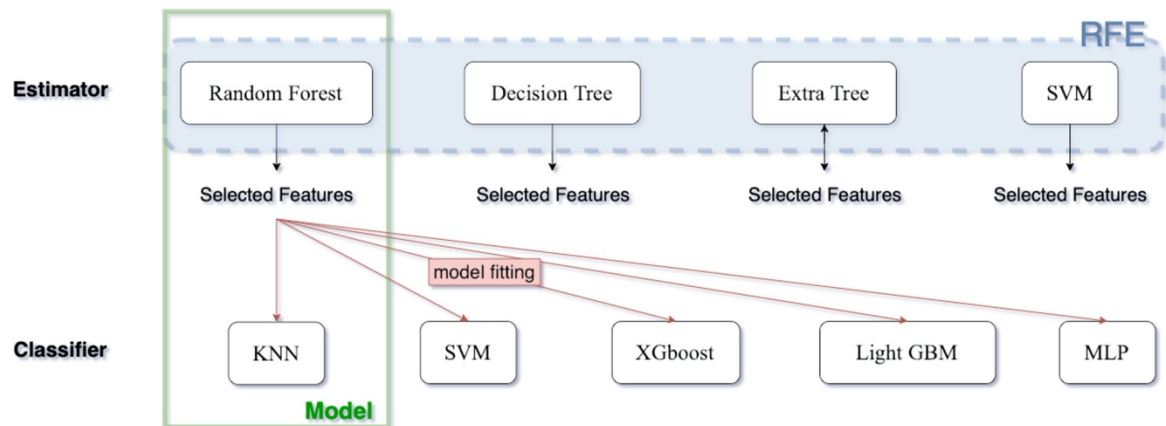


Figure 3 Combination of estimator and classifier

3 Results and Discussions

In this section, we apply our feature selection method to extract important features from the dataset and then analyze the results. The biological meaning of the figure will also be included.

3.1 Extra Tree as the Estimator

In the methodology part, we have mentioned that an overall 20 models are used to look for the best estimator for the RFE algorithm, and the results are as followed. We did the 10 fold cross validation to each of these combined models and same to other paper[50], the accuracy here is based on its performance on the test set. The number of features we first selected is 20 as our novelty here is to look for models with least features but also keep a relatively decent accuracy.

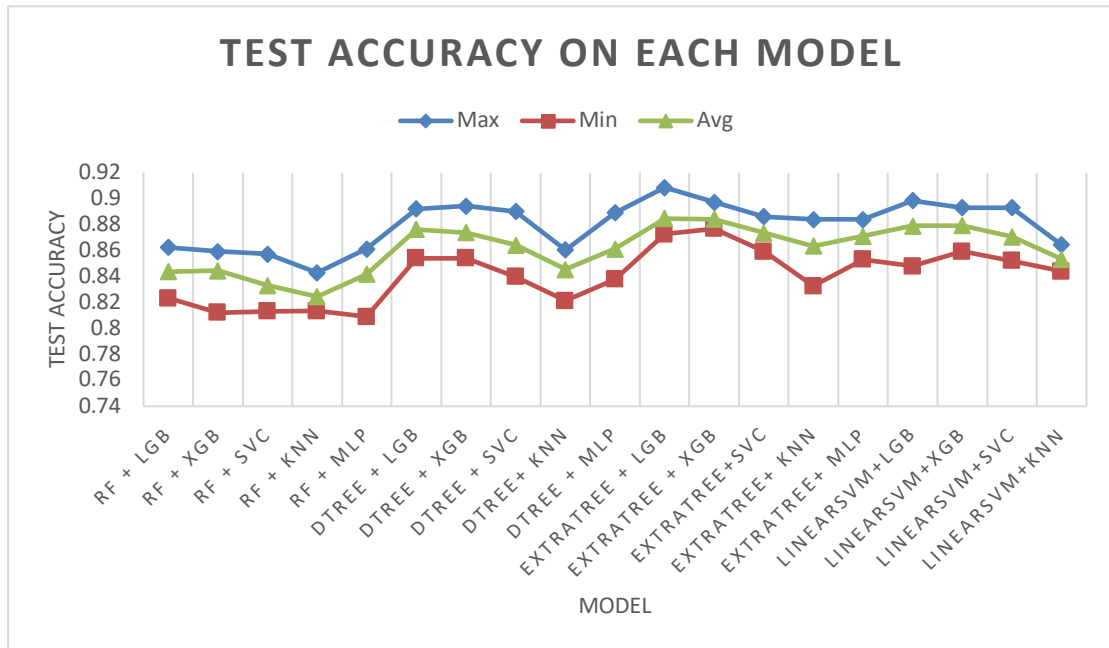


Figure 4 test accuracy on each model

From Figure 4, extra tree algorithm is selected as the estimator of the RFE algorithm since the model with the extra tree have higher 10 cross validation accuracy compared to others. Also, since boosting classifier as lightgbm and xgboost performance well with our model, we additionally test the score of the Catboost classifier [51].

3.2 Model performance for 20 points

We first make our experiment on 20 points since it is the proposed lower bound for our feature numbers. According to 1.1, we obtain the 20 features as below.

Cg08875705	Cg22727783	Cg13668207	Cg05738240	Cg24402880
Cg17853216	Cg12635790	Cg03868944	Cg13709271	Cg14528056
Cg23473955	Cg17295878	Cg17198308	Cg00518941	Cg10706013
Cg08552167	Cg07823492	Cg18368125	Cg27009703	Cg02125316

Table 1 20 selected CpGs

In the research, the sklearn metrics to access the performance of the model includes true positive, true negative, false positive and false negative. Several criteria such as recall score, precision score, f1 score and the overall accuracy will be used as the main indicator for the paper. The task is a multi-class classification, so we choose the parameter 'weighted' to be the key parameter for the indicators since the samples of each class in the dataset is not totally the same. In the following formulas, TP_i represents the number of sample that the truth is class i and the test predicts class i ; TN_i represents the number of sample that the truth is not class i and the test predicts not class i ; FN_i represents the number of sample that the truth is class i but test predicts not class i ; FP_i represents the number of sample that the truth is not class i but test predicts class i [52].

$$Overall_Accuracy = \frac{\sum_{i=1}^{30}(TP_i + TN_i)}{\sum_{i=1}^{30}(TP_i + FP_i + TN_i + FN_i)}$$

$$Precision = \frac{\sum_{i=1}^{30} TP_i}{\sum_{i=1}^{30}(TP_i + FP_i)}$$

$$Recall = \frac{\sum_{i=1}^{30} TP_i}{\sum_{i=1}^{30}(TP_i + FN_i)}$$

$$F1_{score} = \frac{2 \times Precision \times Recall}{Precision + Recall}$$

The overall accuracy is the proportion of correct predictions among the total number of case examined. Precision is the Agreement of the data class labels with those of a classifiers if calculated from sums of per-text decisions. Recall is the Effectiveness of a classifier to identify class labels if calculated from sums of per-text decisions.

. The F_1 score is the harmonic mean of the precision and recall. [52-54]

And then we get the model performance of the three classifiers with only 20 features based on these indicators.

	<i>Overall_Accuracy</i>	<i>Precision</i>	<i>Recall</i>	<i>F1_{score}</i>
CATBOOST	0.91009	0.91866	0.91009	0.91320
LGB	0.89305	0.90163	0.89305	0.89603
XGB	0.89418	0.90156	0.89418	0.89675

Table 2 Compared performance of three classifiers

Thus, the combined model of extra tree plus catboost classifier offer best performance on the dataset and we use this combination to demonstrate the confusion metrics (*Figure 5*).

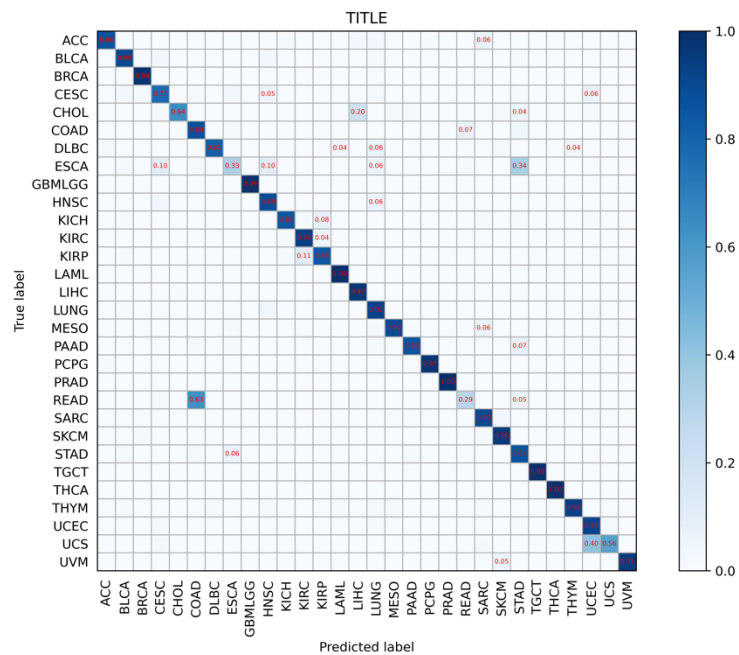


Figure 5 Confusion metrics for 20 points

The element in the diagonal of the matrix represent the sample which can be predicted correctly from the model, and all the other element in the confusion metrics are the wrong predicted samples[55].

From the results, 17 out of 30 classes have the accuracy over 90%, 25 out of 30 classes are able to predict accurately over 80%, however, there still exists some classes which difficult to distinguish between. 34 percent of the ESCA sample are wrongly predicted as STAD, 63 percent of the READ data inaccurately predicted as COAD and 40 percent of the UCS samples falsely predicted as the UCEC.

The imbalanced data set can be one of the factor. Clearly, according to Appendix 1, the sample number we have for UCS is only 57, while UCEC has a relatively larger class at the number of 478, so it may reasonably predicted as the other class which own relatively larger number of data due to the quality of data.

On the other hand, similar to Li(2017)'s work, though they achieve an overall high accuracy on the test set, they still fail to classify three tumor types, such as READ(rectum adenocarcinoma) and COAD(colon adenocarcinoma).

Our team here again showed the difficulty of classifying between READ and COAD class and we may test whether increasing the features can solve the problem in 3.3

3.3 Compared model performance for different feature numbers

Similar to 3.2, we directly use the extra tree as the estimator for the rfe to extract features and use the catboost classifier as the predicting model. The indicators we use here are the same as above and get the result as below(Figure 6)

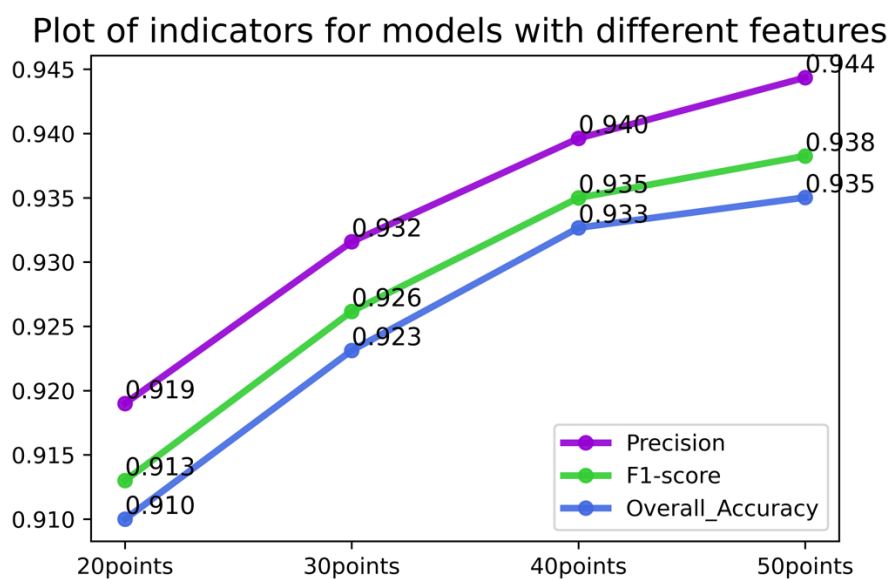


Figure 6

From figure 6 , the performance of the model increases continuously until reaching 40 points, the slope here starts to decrease. Since our aim is to look for the solution with best efficiency (the lowest number of features with high accuracy), we prefer the solution with 40 features. We then analyze the confusion metrics of the models as below (Figure 7, Figure 8 and Figure 9).

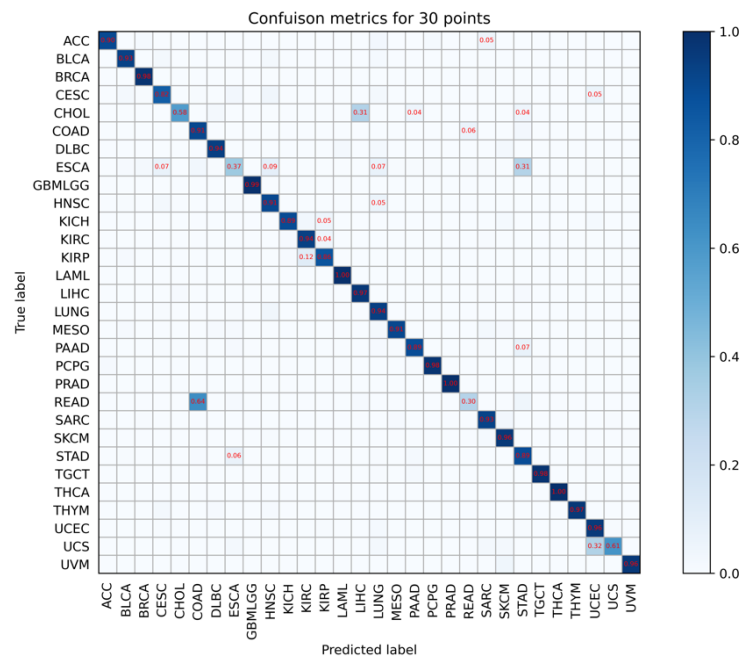


Figure 7 Confusion metrics for 30 features

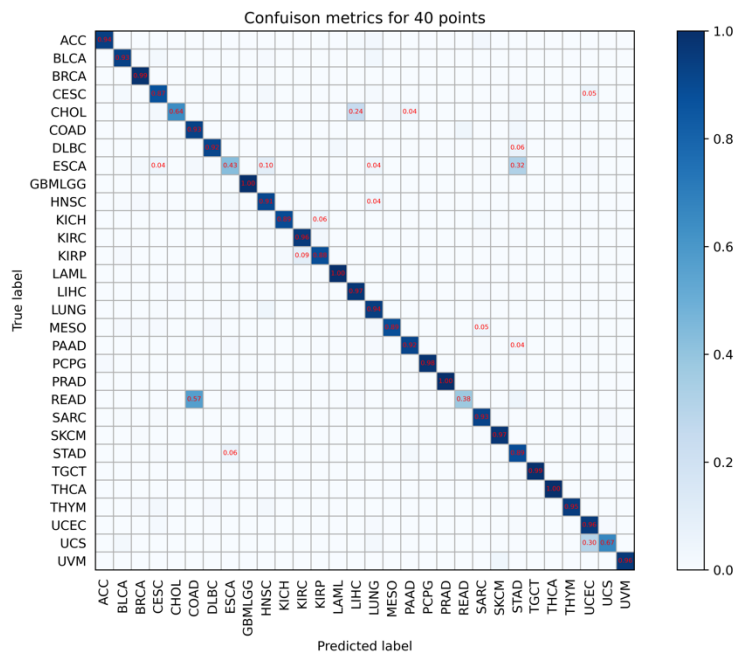


Figure 8 Confusion metrics for 40 features

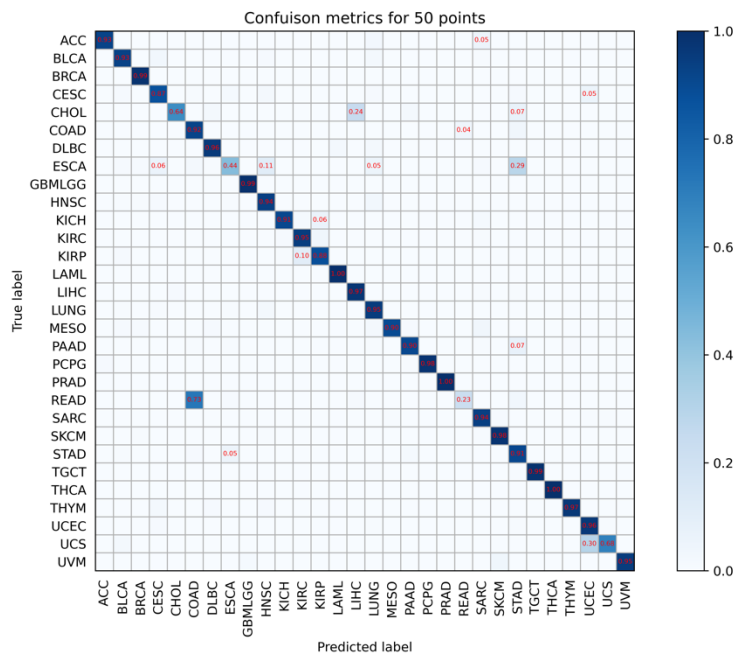


Figure 9 Confusion metrics for 50 features

From those figures, the ambiguity between COAD and READ still exists and not better with the increasing number of features.

The UCS class has an obviously higher accuracy compared to 20 points and so does the ESCA class, so we point out the possibility that these two classes can achieve a decent overall cross-validation accuracy with enough number of features. However, since our paper mainly focuses on classifying these cancer types based on tiny number of features, we will not include further discussion here. Meanwhile, 21 of 30 class with 40 features can achieve accuracy over 0.9 compared to 17 for the 20 features and. In a nutshell, our solution using only 40 identifiers is able to predict the 30 cancer types with 93.3% overall accuracy using the data of DNA methylation 450 values.

3.4 Test robustness of the model

This section works as an inspection for the model, we need to examine the convergence of the RFE algorithm.

3.4.1 RFE Inspection

First, our team examine the intersection of the features. Since RFE algorithm is a backward stepwise selection method which means that the solutions of fewer feature should better be included in the larger feature set. Then we calculate the exact intersection set as followed.

Overlap	30 points	40 points	50 points
For 20 points	20	17	18
For 30 points	/	25	27
For 40 points	/	/	35

Table 3 elements of intersection set

Therefore, the convergence of our model is totally good since the inclusion rate is high. To be mentioned, since the 2000 filtered identifiers need to be reduced to 20, the first twenty selected features should be most robust, then the second twenty

features (20-40). So it is reasonable that the overlapped features of 20 points with the 50 points are greater than the 20 points with the 40 points.

Second, we dive into the performance of the intersection points.

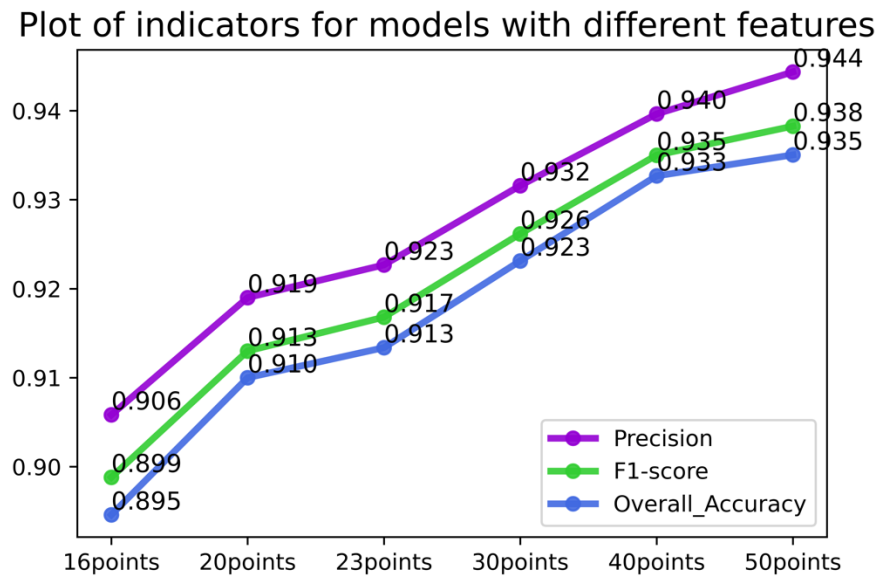


Figure10 Plot of indicators for models consisting of different number of CpGs

From above, it shows that the 16 points solution (the intersection of the 20 points and the 30 points) and the 23 points solution (the intersection of the 30, 40, 50 points) do follow the trend. One point to be noticed is that the indicators decrease for features fewer than 20, which demonstrate that 20 features can be a good starting point for the experiment.

3.5 Genes and biological meaning

3.5.1 Enrichment Analysis

After extracting the identifiers(CpGs) from the data, we map back to find the related genes(Prefix 2) and enrichment analysis has been carried out with DisGeNET[56] and GO Biological Processes [57]by using the *metascape*[58]. Terms with a p-value[59] < 0.01, a minimum count of 3, and an enrichment factor > 1.5 (the enrichment factor is the ratio between the observed counts and the counts expected by chance) are collected and grouped into clusters based on their membership similarities. More specifically, p-values are calculated based on the accumulative hypergeometric

distribution, and q-values are calculated using the Benjamini-Hochberg procedure[60] to account for multiple testings. The results below is the summary of enrichment analysis in DisGeNET

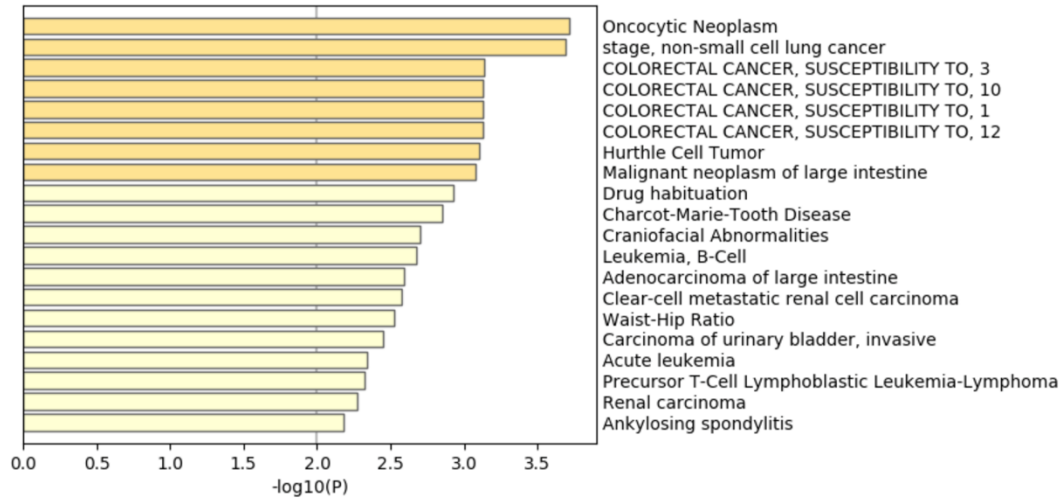


Figure 11 Summary of enrichment analysis in DisGeNET

According to Piñero et al (2019), DisGeNET collected genes and variants associated with human diseases. Therefore, our purpose is to test whether the features we extract by the numerical algorithm have its biological meaning. To be mentioned, since the indicator here is $-\log(P)$, which means that a larger figure leads to a greater significance. Therefore, we identified the first eight diseases in the graph which all turns out to be cancer or related malignant(Oncocytic Neoplasm, Lung Cancer, Colorectal cancer, Thyroid Gland Hurthle (Oncocytic) Cell Neoplasm Hurthle and Malignant Colorectal Neoplasm[61-64]).

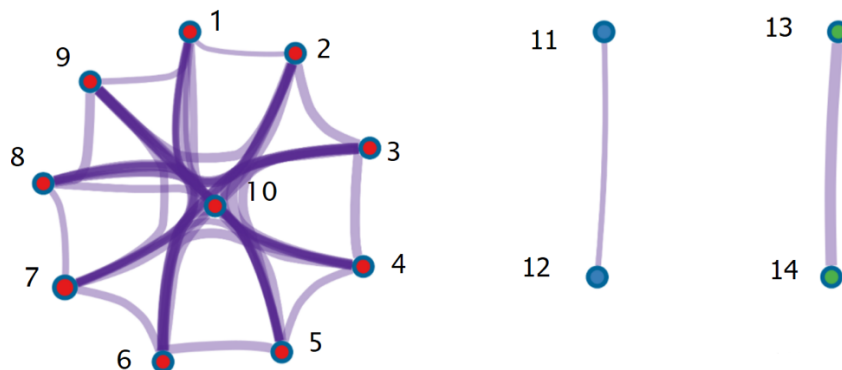


Figure 12 Network of enriched terms colored by cluster ID

Next, we identified all statistically enriched terms accumulative hypergeometric p-values and enrichment factors were calculated and used for filtering. Remaining significant terms were then hierarchically clustered into a tree based on Kappa-statistical similarities among their gene memberships. Then 0.3 kappa score[65] was applied as the threshold to cast the tree into term clusters. We then selected a subset of representative terms from this cluster and convert them into a network layout(figure 6). More specifically, each term is represented by a circle node, where its size is proportional to the number of input genes fall into that term, and its color represent its cluster identity. Terms with a similarity score > 0.3 are linked by an edge[66-67]. As can be seen from figure 6, it is clear that the first polygon gather most terms and thus need a deeper analysis. The table below (Table 3) is the 10 terms in the first polygon and their related LogP value and genes. Genes HOXA9, HOXB1, FGF18, SH3PXD2B and ZMIZ1 are all included in our overlapped 16 features, which biologically support our algorithm.

Node_No	Cluster_id	Hits	LogP
10	32998381	HOXA9 HOXB1 HOXC4 FGF18 SH3PXD2B	-5.383023217
2	32998368	HOXA9 HOXB1 HOXC4 TBX3 FGF18 SH3PXD2B	-4.804057191
3	32998369	HOXA9 HOXB1 HOXC4 TBX3	-4.06992319
4	32998370	HOXA9 HOXB1 HOXC4	-3.815372567
5	32998371	HOXA9 HOXB1 HOXC4 TBX3	-3.535152806
6	32998372	HOXA9 HOXB1 HOXC4	-3.440744804
7	32998373	HOXA9 HOXB1 HOXC4 TBX3 TRIM15	-3.384127137
8	32998374	HOXA9 HOXB1 HOXC4 TBX3	-3.270066923
9	32998375	HOXA9 HOXB1 HOXC4 TBX3 ZMIZ1	-3.241706369
1	32998376	HOXA9 HOXB1 HOXC4 TBX3 ZMIZ1	-3.187787073

Table 4 Detailed information of enriched terms in Figure 12

3.5.2 Gene Annotation

In this section, we will give gene annotations to the overlapped features(intersection of 20, 30, 40, 50 solutions). The genes and corresponding relations with specific cancers are given as follows.

IDENTIFIERS	GENE	CHROM	START	END	RELATED CANCER
CG17198308	IFFO1	chr12	6665329	6665331	GBMLGG
CG17853216	ZMIZ1	chr10	81002479	81002481	GBMLGG, PRAD
CG14528056	GBAP1	chr1	155194781	155194783	STAD
CG07823492	HOXB1	chr17	46608098	46608100	GBMLGG
CG02125316	FGF18	chr5	170878208	170878210	BRCA
CG17295878	TBC1D16	chr17	77924664	77924666	BRCA, SKCM
CG27009703	HOXA9	chr7	27204893	27204895	LUNG
CG03868944	SH3PXD2B	chr5	171808448	171808450	PAAD
CG24402880	PLAC8	chr4	84035836	84035838	COAD,READ
CG00518941	PRKCE	chr2	46361963	46361965	COAD,READ
CG13709271	MARCH8	chr10	45966141	45966143	ESCA
CG08552167	NKX6-2	chr10	134560108	134560110	HNSC

Table 5 12 out of 16 overlapped features have been identified related with cancer

IFFO1-constituted nucleoskeleton prevents chromosome translocation which is a major cause of the onset and progression of diverse types of cancers by immobilizing broken DNA ends during tumorigenesis. Inactivating IFFO1 or its interaction with XRCC4 or lamin A/C leads to increases in both the mobility of broken ends and the frequency of chromosome translocation.[68]

ZMIZ1 gene encodes a member of the PIAS (protein inhibitor of activated STAT) family of proteins. The encoded protein regulates the activity of various transcription factors, including the androgen receptor, Smad3/4, and p53 [69]. Rogers(2013)

demonstrated that the ZMIZ1 might confer selective advantage to tumor cells, which indicated the casual link between ZMIZ1 and tumorigenesis. [70]

GBAP1 is a pseudogene which is defined as nonfunctional gene bearing close resemblance to the known genes at different loci [71]. Research has been conducted to uncover the epigenetic regulation, biological function, and clinical application of GBAP1 in Gastric Cancer risk [72].

HOXB1 plays a important role as an oncogene in diverse tumors as result suggests that HOXB1 gene is a tumor suppressor which is regulated by miR-3175 in Glioma.[73]

FGF18 contributes to breast cancer cells following activation of the Akt/GSK3 β / β -catenin pathway, which makes FGF18 a possible candidate target for breast cancers. [74]

TBC1D16 have been found associated with tumor progression and metastasis in multiple cancer types. Hypomethylation of TBC1D16 was observed in breast cancer and metastatic tumors [75].

SH3PXD2B encodes an adapter protein that is characterized by a PX domain and four Src homology 3 domains [76]. The encoded protein is required for podosome and invadopodia formation and is involved in cell adhesion and migration of numerous cell types. It has been demonstrated that inhibitors of podosome and invadopodia formation might have utility in the treatment of vascular diseases and cancer [77].

HOXA9 which is down-regulated in lung cancer and acts as a tumor progression suppressor is closely related to the aggressive growth of lung cancer cells [78].

HOXA9 contains a homeobox domain that binds to DNA and regulates downstream gene expression [79]. In addition, it is demonstrated that exogenous up-regulation of HOXA9 inhibits tumor cell invasion and migration, inhibits the expression of zinc finger 2 (SNA12/SLUG) by inhibiting the activity of the nuclear factor (NF) - κ B [80].

PRKCE is generally related to the expression of protein kinase C epsilon (PKC ϵ). Encoded by PRKCE, PKC ϵ is an enzyme often related to cell transformation and tumorigenesis. Under the action of PKC ϵ , the Ras/Raf pathway is activated, resulting in the transcription of genes involved in cell proliferation and growth [81].

EPAS1 gene is responsible for the expression of HIF2 α , which is a key component of hypoxia-inducible factor (HIF) associated with the development of tumors in hypoxic conditions. EPAS1 is transcriptionally regulated by DNA methylation in colorectal cancer. Research on EPAS1 have revealed that, for patients with colorectal cancer, there is significant DNA hypermethylation in the EPAS1 regulatory region, which is associated with a decrease in EPAS1 mRNA level in primary cancerous tissues [82]. NKX6B is a murine-homeobox-containing gene localized distally on Chromosome (Chr) 710q26, a region where frequent loss of heterozygosity has been observed in many brain tumors. It is suggested that NKX6B is a possible candidate tumor suppressor gene for brain tumors, particularly for oligodendrogliomas.[83]

PLAC8 is a multi-functional protein that is highly expressed in the intestine, lung, spleen, and innate immune cells, and is involved in various diseases, including cancers, obesity, and innate immune deficiency.[84]

MARCH8 has been shown to down-regulate TNF-related apoptosis inducing ligand receptor 1 (TRAIL-R1) from the cell surface at steady state and possess the potential to provide therapeutic benefit to cancer patients [85]. Additionally, Kumar(2007) identified MARCH8 as one of the differentially expressed gene in esophageal squamous cell carcinoma (ESCC) using 19.1K cDNA microarrays [86] and following the finding Shivam(2017) analyzed its expression and clinical relevance in ESCAs and observed that silencing of MARCH8 affects proliferation, migration/invasion, colony formation potential and apoptosis of ESCC cells. [87]

4 Conclusions and future work

In this research, we succeed in using small number of identifiers in DNA methylation 450k to classify 30 cancer types. We solve the problem of selecting a small subsets of genes from large number of DNA 450K methylated sites, and our parsimonious model is demonstrated to be efficient, achieving an accuracy of 91% , 92.3%, 93.3% and 93.5% for 20, 30, 40 and 50 features respectively. Also, 12 out of 16 of the top

features we select using the framework have been shown implicated in cancer development, which sustain our algorithm biologically. Therefore, our method may act as an auxiliary diagnostic method to determine the actual clinicopathological status of cancer type.

On the other hand, our team also pointed out the problems of distinguishing between COAD(colon adenocarcinoma) and READ(rectum adenocarcinoma) class using the methylation value, which agrees with Li (2017). Since Li uses the RNA-seq data which is somewhat different from us, it is necessary for more research to be done into the area in the future.

Reference

- [1] Robertson K D. DNA methylation and human disease[J]. *Nature Reviews Genetics*, 2005, 6(8): 597-610.
- [2] Moore L D, Le T, Fan G. DNA methylation and its basic function[J]. *Neuropsychopharmacology*, 2013, 38(1): 23-38.
- [3] Baylin, S.B. (2005) DNA methylation and gene silencing in cancer. *Nature Reviews. Clin Oncol*, 2(S1), S4.
- [4] Das P M, Singal R. DNA methylation and cancer[J]. *Journal of clinical oncology*, 2004, 22(22): 4632-4642.
- [5] Pan, Y., Liu, G., Zhou, F., Su, B., & Li, Y. (2018). DNA methylation profiles in cancer diagnosis and therapeutics. *Clinical and experimental medicine*, 18(1), 1-14.
- [6] Baylin S B, Ohm J E. Epigenetic gene silencing in cancer—a mechanism for early oncogenic pathway addiction?[J]. *Nature Reviews Cancer*, 2006, 6(2): 107-116.
- [7] Hahn, W. C. et al. Creation of human tumour cells with defined genetic elements. *Nature* 400, 464–468 (1999).
- [8] Hanahan, D. & Weinberg, R. A. The hallmarks of cancer. *Cell* 100, 57–70 (2000).
- [9] Aaltonen, L. A. et al. Clues to the pathogenesis of familial colorectal cancer. *Science* 260, 812–816 (1993).

-
- [10] Kinzler, K. W. & Vogelstein, B. Lessons from hereditary colorectal cancer. *Cell* 87, 159–170 (1996).
- [11] Kinzler, K. W. & Vogelstein, B. Cancer-susceptibility genes. Gatekeepers and caretakers. *Nature* 386, 761–763 (1997).
- [12] DeVita, V. T., Jr., Lawrence, T. S., & Rosenberg, S. A. (2016). *Cancer : principles & practice of oncology* (10th edition.). Wolters Kluwer.
- [13] *How Cancer Is Diagnosed*. National Cancer Institute. (2019). Retrieved 26 December 2020, from <https://www.cancer.gov/about-cancer/diagnosis-staging/diagnosis>.
- [14] Masilamani, V., Al-Zhrani, K., Al-Salhi, M., Al-Diab, A., & Al-Ageily, M. (2004). *Cancer diagnosis by autofluorescence of blood components*. *Journal of Luminescence*, 109(3-4), 143-154.
- [15] *Understanding Laboratory Tests Fact Sheet*. National Cancer Institute. (2013). Retrieved 26 December 2020, from <https://www.cancer.gov/about-cancer/diagnosis-staging/understanding-lab-tests-fact-sheet>.
- [16] The American Cancer Society medical and editorial content team. (2015). *Imaging (Radiology) Tests for Cancer*. *Cancer.org*. Retrieved 26 December 2020, from <https://www.cancer.org/treatment/understanding-your-diagnosis/tests/imaging-radiology-tests-for-cancer.html>.
- [17] Hao, X. *et al.* DNA methylation markers for diagnosis and prognosis of common cancers. *Proc Natl Acad Sci USA* **114**, 7414–7419 (2017).
- [18] Golub, T. R. *et al.* Molecular Classification of Cancer: Class Discovery and Class Prediction by Gene Expression Monitoring. *Science* **286**, 531–537 (1999).
- [19] Desai AN, Jere A. Next-generation sequencing: ready for the clinics? *Clin Genet.* 81(6): 503-510. (2012)
- [20] Li Y, Kang K, Krahn JM, et al. A comprehensive genomic pan-cancer classification using The Cancer Genome Atlas gene expression data. *BMC Genomics*. 2017;18(1):508. Published 2017 Jul 3. doi:10.1186/s12864-017-3906-0

-
- [21] Zhang S, Wang Y, Gu Y, et al. Specific breast cancer prognosis-subtype distinctions based on DNA methylation patterns. *Mol Oncol.* 2018;12(7):1047-1060. doi:10.1002/1878-0261.12309
- [22] A. A. Raweh, M. Nassef and A. Badr, "A Hybridized Feature Selection and Extraction Approach for Enhancing Cancer Prediction Based on DNA Methylation," in *IEEE Access*, vol. 6, pp. 15212-15223, 2018, doi: 10.1109/ACCESS.2018.2812734.
- [23] Wang, S.-L., Sun, L. & Fang, J. Molecular cancer classification using a meta-sample-based regularized robust coding method. *BMC Bioinformatics* **15**, S2 (2014).
- [24] Roessler, J., Ammerpohl, O., Gutwein, J. *et al.* Quantitative cross-validation and content analysis of the 450k DNA methylation array from Illumina, Inc.. *BMC Res Notes* **5**, 210 (2012). <https://doi.org/10.1186/1756-0500-5-210>
- [25] Darst et al. *BMC Genetics* 2018, 19(Suppl 1):65 <https://doi.org/10.1186/s12863-018-0633-8>
- [26] The Cancer Genome Atlas Program. Retrieved 18 July 2020, from <https://www.cancer.gov/about-nci/organization/ccg/research/structural-genomics/tcga>
- [27] UCSC Xena. Retrieved 18 July 2020, from <https://xenabrowser.net/datapages/?host=https%3A%2F%2Ftcga.xenahubs.net&removeHub=https%3A%2F%2Fxena.treehouse.gi.ucsc.edu%3A443>
- [28] Du, P., Zhang, X., Huang, C. C., Jafari, N., Kibbe, W. A., Hou, L., & Lin, S. M. (2010). Comparison of Beta-value and M-value methods for quantifying methylation levels by microarray analysis. *BMC bioinformatics*, 11(1), 587.
- [29] Illumina. (2012). *Infinium® HumanMethylation450 BeadChip*. Retrieved from https://www.illumina.com/content/dam/illumina-marketing/documents/products/datasheets/datasheet_humanmethylation450.pdf

-
- [30] Dedeurwaerder, S., Defrance, M., Bizet, M., Calonne, E., Bontempi, G., & Fuks, F. (2014). A comprehensive overview of Infinium HumanMethylation450 data processing. *Briefings in bioinformatics*, 15(6), 929–941.
<https://doi.org/10.1093/bib/bbt054>
- [31] Sandoval, J., Heyn, H., Moran, S., Serra-Musach, J., Pujana, M. A., Bibikova, M., & Esteller, M. (2011). Validation of a DNA methylation microarray for 450,000 CpG sites in the human genome. *Epigenetics*, 6(6), 692-702.
- [32] Joubert Boniie R.et al. 450K Epigenome-Wide Scan Identifies Differential DNA Methylation in Newborns Related to Maternal Smoking during Pregnancy. *Environmental Health Perspectives*, [s.l.], v.120, n.10,p.1425-1431, 2012
- [33] Sarkar,S.et al. Array-based DNA methylation profiling reveals peripheral blood diferential methylation in male infertility. *Fertility and Sterility*, [s.l.], v.122, n.1, p.61-72, 2019
- [34] Why, How and When to apply Feature Selection. (2018). Retrieved 25 July 2020, from <https://towardsdatascience.com/why-how-and-when-to-apply-feature-selection-e9c69ad-fabf2>
- [35] Guyon, I., Weston, J., Barnhill, S. and Vapnik, V. J. M. I. Gene selection for cancer classification using support vector machines, 46, 1-3 (2002), 389-422.
- [36] Y. Tang, Y. Zhang and Z. Huang, "Development of Two-Stage SVM-RFE Gene Selection Strategy for Microarray Expression Data Analysis," in *IEEE/ACM Transactions on Computational Biology and Bioinformatics*, vol. 4, no. 3, pp. 365-381, July-Sept. 2007, doi: 10.1109/TCBB.2007.1028.
- [37] Majid Afshar, Hamid Usefi, arXiv:2002.12104 [cs.LG], 2020
- [38] Fabian Model, Péter Adorján, Alexander Olek, Christian Piepenbrock, Feature selection for DNA methylation based cancer classification , *Bioinformatics*, Volume 17, Issue suppl_1, June 2001, Pages S157–S164, https://doi.org/10.1093/bioinformatics/17.suppl_1.S157
- [39] Deng, H. & Runger, G. Feature Selection via Regularized Trees. *arXiv:1201.1587 [cs, stat]* (2012).

-
- [40] Touw, W. G. et al. (2013) Data Mining in the life sciences with random forest: a walk in the park or lost in the jungle? *Brief. Bioinformatics*, 14, 315-216
- [41] Breiman, L., Friedman, J., Stone, C. J. and Olshen, R. A. *Classification and regression trees*. CRC press, 1984.
- [42] Geurts, P., Ernst, D. and Wehenkel, L. J. M. I. Extremely randomized trees, 63, 1 (2006), 3-42.
- [43] Moon, M. & Nakai, K. Stable feature selection based on the ensemble L₁-norm support vector machine for biomarker discovery. *BMC Genomics* **17**, 1026 (2016).
- [44] Sahu, B., Dehuri, S. & Jagadev, A. K. Feature selection model based on clustering and ranking in pipeline for microarray data. *Informatics in Medicine Unlocked* **9**, 107–122 (2017).
- [45] Suykens, J. A. K. and Vandewalle, J. Least Squares Support Vector Machine Classifiers. *Neural Processing Letters*, 9, 3 (06// 1999), 293.
- [46] Keller, J. M., Gray, M. R., Givens, J. A. J. I. t. o. s., man, and cybernetics A fuzzy k-nearest neighbor algorithm, 4 (1985), 580-585.
- [47] Ruck, D. W., Rogers, S. K. and Kabrisky, M. J. J. o. N. N. C. Feature selection using a multilayer perceptron, 2, 2 (1990), 40-48.
- [48] Ke, G., Meng, Q., Finley, T., Wang, T., Chen, W., Ma, W., Ye, Q. and Liu, T.-Y. *Lightgbm: A highly efficient gradient boosting decision tree*. City, 2017.
- [49] Chen, T. and Guestrin, C. *Xgboost: A scalable tree boosting system*. City, 2016.
- [50] Sklearn.feature_selection.RFE. Retrieved 27 July 2020, from https://scikitlearn.org/stable/modules/generated/sklearn.feature_selection.RFE.html
- [46] Prokhorenkova, L., Gusev, G., Vorobev, A., Dorogush, A. V. & Gulin, A. CatBoost: unbiased boosting with categorical features. 11.
- [47] Fawcett, Tom (2006). "An Introduction to ROC Analysis" (PDF). *Pattern Recognition Letters*. 27 (8): 861–874. doi:10.1016/j.patrec.2005.10.010.

-
- [48] Powers, David M W (2011). "Evaluation: From Precision, Recall and F-Measure to ROC, Informedness, Markedness & Correlation". *Journal of Machine Learning Technologies*. 2 (1): 37–63.
- [49] Marina Sokolova a,* , Guy Lapalme b, A systematic analysis of performance measures for classification tasks, *Information Processing and Management*, 45 (2009) 427–437
- [50] Visa, S., Ramsay, B. & Ralescu, A. Confusion Matrix-based Feature Selection. 8.
- [51] Piñero, J., Ramírez-Anguita, J. M., Saüch-Pitarch, J., Ronzano, F., Centeno, E., Sanz, F. and Furlong, L. I. The DisGeNET knowledge platform for disease genomics: 2019 update. *Nucleic Acids Research*, 48, D1 (2020), D845-D855.
- [52] Hill, D.P., Smith, B., McAndrews-Hill, M.S. *et al.* Gene Ontology annotations: what they mean and where they come from. *BMC Bioinformatics* 9, S2 (2008).
<https://doi.org/10.1186/1471-2105-9-S5-S2>
- [53] Zhou et al., Metascape provides a biologist-oriented resource for the analysis of systems-level datasets. *Nature Communications* (2019) 10(1):1523.
- [54] Nuzzo, R. J. N. N. Scientific method: statistical errors, 506, 7487 (2014), 150.
- [55] Benjamini, Y. and Hochberg, Y. J. J. o. t. R. s. s. B. Controlling the false discovery rate: a practical and powerful approach to multiple testing, 57, 1 (1995), 289-300.
- [56] Wilkins T, McMechan D, Talukder A. Colorectal Cancer Screening and Prevention. *Am Fam Physician*. 2018 May 15;97(10):658-665. PMID: 29763272.
- [57] Grani G, Lamartina L, Durante C, Filetti S, Cooper DS. Follicular thyroid cancer and Hürthle cell carcinoma: challenges in diagnosis, treatment, and clinical management. *Lancet Diabetes Endocrinol*. 2018 Jun;6(6):500-514. doi: 10.1016/S2213-8587(17)30325-X. Epub 2017 Nov 5. PMID: 29102432.
- [58] Herbst RS, Morgensztern D, Boshoff C. The biology and management of non-small cell lung cancer. *Nature*. 2018 Jan 24;553(7689):446-454. doi: 10.1038/nature25183. PMID: 29364287.

-
- [59] Mearini L, Del Sordo R, Costantini E, Nunzi E, Porena M. Adrenal oncocytic neoplasm: a systematic review. *Urol Int.* 2013;91(2):125-33. doi: 10.1159/000345141. Epub 2012 Nov 8. PMID: 23147196.
- [60] Cohen, J. J. E. and measurement, p. A coefficient of agreement for nominal scales, 20, 1 (1960), 37-46.
- [61] Carpentier, M., Combescure, C., Merlini, L. and Perneger, T. V. J. B. m. r. m. Kappa statistic to measure agreement beyond chance in free-response assessments, 17, 1 (2017), 62.
- [62] Cantor, A. B. J. P. m. Sample-size calculations for Cohen's kappa, 1, 2 (1996), 150.
- [63] Li, W. et al. (2019) 'The nucleoskeleton protein IFFO1 immobilizes broken DNA and suppresses chromosome translocation during tumorigenesis', *Nature Cell Biology*, 21(10), p. 1273. doi: 10.1038/s41556-019-0388-0.
- [64] Li, X., Thyssen, G., Beliakoff, J., Sun, Z., 2006. The Novel PIAS-like Protein hZimp10 Enhances Smad Transcriptional Activity. *Journal of Biological Chemistry*.. doi:10.1074/jbc.m508365200
- [65] Rogers, L. M., Riordan, J. D., Swick, B. L., Meyerholz, D. K. & Dupuy, A. J. Ectopic Expression of Zmiz1 Induces Cutaneous Squamous Cell Malignancies in a Mouse Model of Cancer. *Journal of Investigative Dermatology* 133, 1863–1869 (2013).
- [66] Sur S, Saha S, Tisa LS, et al. Characterization of pseudogenes in members of the order Frankineae. *J Biosciences.* 2013;38:727-732.
- [67] Ma, G. et al. A genetic variation in the CpG island of pseudogene GBAP1 promoter is associated with gastric cancer susceptibility. *Cancer* 125, 2465–2473 (2019).
- [68] Han, L., Liu, D., Li, Z., Tian, N., Han, Z., Wang, G., Fu, Y., Guo, Z., Zhu, Z., Du, C., & Tian, Y. (2015). HOXB1 Is a Tumor Suppressor Gene Regulated by miR-3175 in Glioma. *PloS one*, 10(11), e0142387. <https://doi.org/10.1371/journal.pone.0142387>
- [69] Song N, Zhong J, Hu Q, Gu T, Yang B, Zhang J, Yu J, Ma X, Chen Q, Qi J, Liu Y, Su W, Feng Z, Wang X, Wang H. FGF18 Enhances Migration and the Epithelial-Mesenchymal Transition in Breast Cancer by Regulating Akt/GSK3 β /B-Catenin

Signaling. *Cell Physiol Biochem*. 2018;49(3):1019-1032. doi: 10.1159/000493286.

Epub 2018 Sep 7. PMID: 30196303.

[70] Rodger, E.J., Chatterjee, A., Stockwell, P.A. et al. Characterisation of DNA methylation changes in EBF3 and TBC1D16 associated with tumour progression and metastasis in multiple cancer types. *Clin Epigenet* 11, 114 (2019).

<https://doi.org/10.1186/s13148-019-0710-5>

[71] Lányi Á, Baráth M, Péterfi Z, et al. The homolog of the five SH3-domain protein (HOFl/SH3PXD2B) regulates lamellipodia formation and cell spreading. *PLoS One*.

2011;6(8):e23653. doi:10.1371/journal.pone.0023653

[72] Courtneidge SA. Cell migration and invasion in human disease: the Tks adaptor proteins. *Biochem Soc Trans*. 2012;40(1):129-132. doi:10.1042/BST20110685

[73] Son, J. W. et al. (2011) 'Genome-wide combination profiling of DNA copy number and methylation for deciphering biomarkers in non-small cell lung cancer patients', *Cancer Letters*, 311(1), pp. 29–37. doi: 10.1016/j.canlet.2011.06.021.

[74] LaRonde-LeBlanc, N. A. (1,3) and Wolberger, C. (1,2) (no date) 'Structure of HoxA9 and Pbx1 bound to DNA: Hox hexapeptide and DNA recognition anterior to posterior', *Genes and Development*, 17(16), pp. 2060–2072. doi:

10.1101/gad.1103303.

[75] Yu, S.-L. et al. (2019) 'Recombinant cell-permeable HOXA9 protein inhibits NSCLC cell migration and invasion', *Cellular Oncology (2211-3428)*, 42(3), pp. 275–285. doi: 10.1007/s13402-019-00424-4.

[76] Zhang, X., Li, D., Li, M., Ye, M., Ding, L., Cai, H., ... & Lv, Z. (2014). MicroRNA-146a targets PRKCE to modulate papillary thyroid tumor development. *International journal of cancer*, 134(2), 257-267.

[77] Rawłuszko-Wieczorek, A. A., Horbacka, K., Krokowicz, P., Misztal, M., & Jagodziński, P. P. (2014). Prognostic potential of DNA methylation and transcript levels of HIF1A and EPAS1 in colorectal cancer. *Molecular cancer research*, 12(8), 1112-1127.

-
- [78] Lee, H. et al. (2018) 'CRISPR/Cas9-mediated generation of a Plac8 knockout mouse model', *Laboratory Animal Research*, 34(4), p. 279. doi: 10.5625/lar.2018.34.4.279.
- [79] Li, C. et al. (2014) 'Excess PLAC8 promotes an unconventional ERK2-dependent EMT in colon cancer', *Journal of Clinical Investigation*, (5), p. 2172. doi: 10.1172/JCI71103.
- [80] Van de Kooij, B. et al. Ubiquitination by the Membrane-associated RING-CH-8 (MARCH-8) Ligase Controls Steady-state Cell Surface Expression of Tumor Necrosis Factor-related Apoptosis Inducing Ligand (TRAIL) Receptor 1. *J. Biol. Chem.* 288, 6617–6628 (2013).
- [81] Kumar A, Chatopadhyay T, Raziuddin M, Ralhan R. Discovery of deregulation of zinc homeostasis and its associated genes in esophageal squamous cell carcinoma using cDNA microarray. *Int J Cancer.* 2007;120:230–42.
- [82] Singh, S., Saraya, A., Das, P. & Sharma, R. Increased expression of MARCH8, an E3 ubiquitin ligase, is associated with growth of esophageal tumor. *Cancer Cell Int* 17, 116 (2017).

APPENDIX

Appendix 1 : Number of samples in each class

Dataset	No. of samples
ACC	80
BLCA	434
BRCA	888
CESC	312
CHOL	45
COAD	337
DLBC	48
ESCA	202

GBMLGG	685
HNSC	580
KICH	66
KIRC	480
KIRP	321
LAML	194
LIHC	429
LUNG	907
MESO	87
PAAD	195
PCPG	187
PRAD	549
READ	106
SARC	269
SKCM	476
STAD	398
TGCT	156
THCA	571
THYM	126
UCEC	478
UCS	57
UVM	80

Appendix 2

#id	gene	chrom	chromStart	chromEnd	Importance
cg17198308	IFFO1	chr12	6665107	6665109	.
cg10706013	PDE9A	chr21	44104949	44104951	.
cg05738240	RBM19,TRNA_Pseudo	chr12	114337926	114337928	.

cg22727783	TRIO,FAM105A	chr5	14441073	14441075	.
cg14528056	GBAP1	chr1	155194781	155194783	Overlapped
cg24402880	PLAC8	chr4	84035836	84035838	Overlapped
cg17853216	ZMIZ1	chr10	81002479	81002481	Overlapped
cg07823492	HOXB1	chr17	46608098	46608100	Overlapped
cg13668207	BC043551	chr12	65904451	65904453	Overlapped
cg17295878	TBC1D16	chr17	77924664	77924666	Overlapped
cg23473955	ABHD15	chr17	27893406	27893408	Overlapped
cg00518941	PRKCE,EPAS1	chr2	46361963	46361965	Overlapped
cg08552167	INPP5A,NKX6-2	chr10	134560108	134560110	Overlapped
cg27009703	HOXA9	chr7	27204893	27204895	Overlapped
cg13709271	MARCH8,40976	chr10	45966141	45966143	Overlapped
cg08875705	IFFO1	chr12	6665329	6665331	Overlapped
cg12635790	MIR3150B	chr8	96112813	96112815	Overlapped
cg18368125	TMED6	chr16	69385826	69385828	Overlapped
cg03868944	SH3PXD2B	chr5	171808448	171808450	Overlapped
cg02125316	FGF18	chr5	170878208	170878210	Overlapped
cg08913523	Mir_544	chr8	126649806	126649808	.
cg04770088	RGS9	chr17	63225019	63225021	.
cg00363813	IFFO1	chr12	6664871	6664873	.
cg23089272	FSIP1	chr15	39985430	39985432	.
cg06627617	ASAP2,ITGB1BP1	chr2	9471178	9471180	.
cg17806482	LAMB1,U3	chr7	107608006	107608008	.
cg05327192	KLHL35	chr11	75133592	75133594	.
cg14723977	WIZ,AKAP8L	chr19	15532805	15532807	.
cg17785786	CPE,JA611274	chr4	166414665	166414667	.
cg18920088	MTHFD1L,U6	chr6	151346408	151346410	.
cg27285599	ZNF750,TBCD	chr17	80798022	80798024	.
cg02989244	MPP7	chr10	28657269	28657271	.
cg07786675	SFN	chr1	27189984	27189986	.
cg06132620	NHSL1	chr6	138820502	138820504	.
cg09053536	TBX3	chr12	115117550	115117552	.
cg27514336	NEK11,NUDT16P1	chr3	131068940	131068942	.
cg01979888	IFFO1	chr12	6665423	6665425	.
cg16783204	AK055272	chr16	89119370	89119372	.
cg04340430	LOC440839,AK123617	chr2	113967478	113967480	.

cg15912800	MIR196B	chr7	27209196	27209198	.
cg16953816	VPS37B,HIP1R	chr12	123349951	123349953	.
cg26654807	ZMIZ1	chr10	81002217	81002219	.
cg10704263	CYTH1	chr17	76732904	76732906	.
cg24425838	LOC100132111,C2CD4D	chr1	151812434	151812436	.
cg27138204	HOXC4	chr12	54446099	54446101	.
cg12904880	TRIM15	chr6	30139831	30139833	.
cg08145381	KIAA0317,SNORA7	chr14	75172504	75172506	.
cg03025986	TSSC1	chr2	3292756	3292758	.
cg13630878	MTMR15,FAN1	chr15	31215821	31215823	.
cg22202558	CUX1	chr7	101500302	101500304	.
cg05002406	PDLIM3	chr4	186425753	186425755	.
cg22455450	ZNF808	chr19	53038971	53038973	.
cg19794481	MIR141	chr12	7073239	7073241	.
cg25599924	ACOX3	chr4	8396055	8396057	.
cg15958289	DCPS	chr11	126188993	126188995	.
cg19483007	WWTR1,AK309441	chr3	149327650	149327652	.

Appendix 2. CpGs and related genes in this study

(Illumina Methylation450k Gene Mapping can be achieved by

https://tcga.xenahubs.net/download/probeMap/illuminaMethyl450_hg19_GPL1630

4_TCGAlegacy)

Appendix 3

MODEL	Estimator	Classifier	Max	Min	Avg
1	Random Forest	LGB	0.86256	0.82341	0.84389
2	Random Forest	XGBOOST	0.85934	0.81211	0.84461
3	Random Forest	SVC	0.85744	0.81314	0.83311
4	Random Forest	KNN	0.84292	0.81333	0.82449
5	Random Forest	MLP	0.8614	0.80903	0.84184
6	Decision Tree	LGB	0.8922	0.85421	0.87632
7	Decision Tree	XGBOOST	0.89425	0.85421	0.87396
8	Decision Tree	SVC	0.89014	0.83984	0.86421

9	Decision Tree	KNN	0.86051	0.82136	0.84553
10	Decision Tree	MLP	0.88912	0.83778	0.86134
11	Extra Tree	LGB	0.90862	0.87269	0.88463
12	Extra Tree	XGBOOST	0.89733	0.8768	0.88433
13	Extra Tree	SVC	0.88615	0.85934	0.87355
14	Extra Tree	KNN	0.88398	0.83265	0.86349
15	Extra Tree	MLP	0.8841	0.85318	0.87108
16	Linear SVM	LGB	0.89862	0.84805	0.87909
17	Linear SVM	XGBOOST	0.89862	0.84805	0.87909
18	Linear SVM	SVC	0.89322	0.85934	0.8792
19	Linear SVM	KNN	0.89322	0.85216	0.87068
20	Linear SVM	MLP	0.86448	0.8441	0.85333

Appendix 3 Model performance of 10 fold cross-validation Accuracy